Zahn, R., Comas, M.C., and Klaus, A. (Eds.), 1999
Proceedings of the Ocean Drilling Program, Scientific Results, Vol. 161

21. FISSION-TRACK ANALYSIS OF SAMPLES FROM THE ALBORAN SEA BASEMENT[1]

Anthony J. Hurford,[2] John P. Platt,[2] and Andrew Carter[2]

ABSTRACT

Fission-track analysis was used to examine 13 basement samples of high-grade schist, pelitic gneiss, granite, migmatite, and calc-silicate rock, obtained from Ocean Drilling Program Hole 976B in the floor of the Alboran Sea. Long mean-track-length and tight length distributions, together with homogeneity of apatite age, indicate rapid cooling through the temperature range from 120° to 60°C at about 18–19 Ma. This cooling history represents exhumation within the top few kilometers of the earth's surface, and is therefore likely to date the creation of the present basement morphology in the area. The cooling age is very close to the age of the oldest sediments in the Alboran Sea, which indicates a close link in time between basement exhumation and creation of the Alboran Sea basin.

INTRODUCTION

The Alboran Sea is an extensional basin of late Tertiary age that formed in close association with the Betic-Rif thrust belt in adjacent regions of southern Spain and Morocco. Leg 161 of the Ocean Drilling Program established that the basement underlying the Neogene sediments of the basin is made up of high-grade metamorphic rocks very similar to those in nearby regions of the Betic Cordillera (Shipboard Scientific Party, 1996). This appears to confirm the hypothesis that the Alboran Sea formed by the extensional collapse of a collisional orogen that previously occupied the region (Platt and Vissers, 1989). The exhumation history of the basement is therefore of crucial importance to understanding the timing and mechanism of basin formation. This paper presents the results of fission-track (FT) analyses of apatite from basement rock that was cored at Site 976. The primary objective of the analyses was to determine the low-temperature thermal history of the basement, as an aid in determining the timing and rate of exhumation.

Site 976 is located at 36°12.3′N, 4°18.8′W, in the Alboran Sea, 60 km south of Málaga in southern Spain (Shipboard Scientific Party, 1996). It lies on a basement high in the West Alboran Basin that was created by normal faulting, probably in early to middle Miocene time (Comas et al., 1992; Watts et al., 1993), but which is now completely buried beneath Miocene–Holocene sediment. The crustal thickness in the area is probably between 15 and 20 km (Working Group, 1978). In Hole 976B, the basement is covered unconformably by 670 m of sediment of Serravallian (nannoplankton zone NN7, middle Miocene) to Pleistocene age (Shipboard Scientific Party, 1996), which places a younger age limit of 11–12 Ma on the exhumation of the metamorphic rocks.

The top 124 m of the basement core from Hole 976B consists of high-grade pelitic schist with interlayers of carbonate and calc-silicate rocks. This passes down into a massive pelitic gneiss, which is locally migmatitic, with irregular veins and segregations of granitic material. The petrology of both rock types suggests that they reached peak temperatures above 650°C, and remained at high temperature to very low pressures, of the order of 4 kbar or less (Platt et al., 1996; Shipboard Scientific Party, 1996; Soto et al., Chap. 19, this volume; Soto et al., in press).

METHODOLOGY

Spontaneous fission decay of ^{238}U present in apatite produces minute damage tracks in the crystal lattice that can be seen using an optical microscope. The number of these fission tracks reveals the time over which the tracks have been accumulating. Sensitivity of fission tracks to temperature results in significant track shortening (annealing) at temperatures above ~60°C over geological time. Measuring track lengths provides an estimation of temperature through use of the empirically derived track shortening-to-temperature relationship. In combination, FT apatite age and track-length data can provide a quantitative estimate of the low-temperature (<120°C) thermal history of a rock.

Apatite, where present, was separated from the core samples by conventional crushing, sieving, and magnetic and heavy-liquid separation techniques. Apatite grain mounts were prepared by using epoxy resin on a glass slide and then polishing using carbide papers and alumina. Tracks from spontaneous fission of ^{238}U were revealed by etching with 5-N HNO_3 at 20°C for 20 s. Uranium contents of the samples were assessed by irradiating with thermal (low-energy) neutrons, which induce fission in a proportion of ^{235}U sample atoms. The induced tracks were recorded in an external detector of mica, clamped against the sample during irradiation (Gleadow, 1981). Samples were irradiated in the D-3 thermal facility of the Risø Reactor, National Research Center, Roskilde, Denmark, where the cadmium ratio (thermal/epithermal + fast neutrons) is >400, which is well-suited to FT use (Green and Hurford, 1984). Neutron fluence (or time-integrated neutron flux) was monitored using a Corning glass dosimeter CN-5, with a known uranium content of 11 ppm (Hurford and Green, 1982). After irradiation, sample and dosimeter mica detectors were etched in 40% hydrofluoric acid at 20°C for 45 min.

Spontaneous ^{238}U and induced ^{235}U fission track densities were counted for individual apatites in the crystal and its mirror-imaged impression in the mica detector, respectively. Zeiss Axioplan microscopes with 100× dry objectives and a total magnification of 1250× were used for counting. Only crystals with prismatic sections parallel to the *c*-crystallographic axis, and hence high etching efficiencies, were analyzed: the appropriate geometry factor between spontaneous and induced track densities in this case is 0.5. To avoid a bias in the results through selection of apatite crystals, each sample was systematically scanned, and each crystal that was encountered with the correct orientation was analyzed, regardless of the track density.

The IUGS-recommended zeta calibration approach was used to calculate the ages, whereby a proportionality or calibration constant zeta is evaluated by multiple analysis of mineral standards of known

[1]Zahn, R., Comas, M.C., and Klaus, A. (Eds.), 1999. *Proc. ODP, Sci. Results,* 161: College Station, TX (Ocean Drilling Program).

[2]Research School of Geological and Geophysical Sciences, University College London and Birkbeck College, Gower Street, London WC1E 6BT, United Kingdom. John.Platt@ucl.ac.uk

age (Hurford and Green, 1983). The zeta value of 339 ± 5 for dosimeter glass CN-5 has been derived by analyst Andrew Carter from 33 determinations of apatites from the Fish Canyon Tuff, Colorado; the Durango deposit, Cerro de Mercado, Mexico; and the Mount Dromedary banatite, New South Wales, Australia (Hurford, 1990).

A Houston Instruments digitizing tablet was used to measure horizontally confined FT lengths in the apatite crystals, with a cursor equipped with a high-intensity, red-light–emitting diode (LED). The image of the LED, viewed in the microscope via a drawing tube attachment, was superimposed on either end of the track in turn, and the X and Y coordinates for each track end recorded on the tablet. Calibration of the tablet against a stage micrometer provided a direct measure of each track length with an overall precision of about ± 0.1 μm.

RESULTS

Table 1 lists the analytical details of the FT data measured for samples from Hole 976B together with the calculated ages, and the means and standard deviations of the track-length distributions. Sample 161-77R-2 (Piece 3B), failed to yield adequate apatite grains for analysis, whereas high numbers of inclusions that were found in apatite from Sample 83R-1 (Piece 11A), precluded confident identification of fission tracks.

Ages are central ages, modal ages weighted to account for the difference in precision of the individual crystal ages within a sample analysis. Two uncertainties attach to the central age: (1) the ± indicates analytical precision (derived from the numbers of tracks counted); and (2) the age dispersion signifies the spread of the individual crystal ages and tests if a single population is present. The significance of the age data is clearer on a radial plot (Galbraith, 1990), which is a graphical method for comparing crystals of different ages and precisions. Figure 1 shows radial plots of this type, as well as histograms of the single-crystal age data from Site 976, and confined track-length distributions for each sample analyzed in this study. The position on the x-scale in the radial plots records the uncertainty of individual age estimates, whereas each point has the same standard error on the y-scale (illustrated as ± 2σ). In essence, the further the data point plots from the origin, the more precise the measurement. The age of each crystal may be determined by extrapolating a line from the origin at the left of the plot through the crystal's x and y coordinates to intercept the age scale. The spread of single-crystal ages in each sample is very small: the indices of age dispersion show, in each case, relative errors <10% and P(χ^2) values >5% (Table 1), which indicate that all analyzed grains are derived from a single population and have a common age with only Poissonian variation (Galbraith, 1981; Galbraith and Laslett, 1993). Such homogeneity of age suggests a relatively simple thermal history. Measured apatite central ages range between 15.2 ± 1.3 Ma and 21.4 ± 2.3 Ma (± 1σ) for samples drilled over a vertical distance of ~115 m. Plots of relative sample depth vs. measured ages (Fig. 2A) and mean track lengths (Fig. 2B) show overlapping results, which, at 95% confidence limits, are indistinguishable among samples.

DISCUSSION

The length of fission tracks in apatite provide the means of interpreting age: each length represents a different portion of the time-temperature history (tT) story, and length distributions record the integrated thermal history. In the data from Site 976 there is a high degree of similarity of track-length data with mean track lengths (MTL) that range from 14.78 ± 0.21 μm to 13.83 ± 0.24 μm and standard deviations from 0.83 to 1.29 (Table 1). Distributions shown in Figure 1 also indicate an absence of short tracks <10 μm (except Sample 161-97R-2 (Piece 1), the sample with the shortest MTL). Long track lengths (>14.5 μm) and tight distributions are characteristic of rapid cooling, such as found in thermally undisturbed volcanic rocks (Gleadow et al., 1986). The track-length data, together with the homogeneous, low-dispersion ages, provide strong evidence for rapid cooling of the Site 976 samples from temperatures above total track annealing to temperatures <60°C at the time given by measured age: ~18–19 Ma.

Numerical modeling of the data has used a form of Monte Carlo simulation to select four time-temperature points from within the bounds 30 ± 30 Ma and 60° ± 60°C. This thermal history, together with a present-day temperature of 30° ± 10°C, was used to predict FT parameters. Those predictions were then quantitatively compared to the observed values. Time-temperature points were selected randomly to start with, after which a genetic algorithm was used (Gallagher, 1995). A total of 5000 thermal histories were tested. Figure 3A shows the ten modeled runs whose predicted track ages and length parameters fit best with the measured values. In each case the passage through the partial annealing zone (PAZ) is similar, with cooling from 120° to 60°C in about 2 Ma. Figure 3B shows the overall best-fit modeled run, which shows a very close agreement between measured and predicted length distributions and ages. (Note that the subsequent variation at temperatures <60°C is irrelevant because no significant track annealing occurs at these temperatures.)

Details of thermal history are often revealed where individual samples yield differences in measured age and track length. Each sample at a different crustal level in effect preserves an individual record of part of the overall regional thermal history (e.g., see Lewis et al., 1992). Similar plots of the age and length data measured for the Site 976 samples (Fig. 4) show no such trends, which argues against complexity and favors a relatively simple thermal history. Although the samples come from within a faulted and fault-bounded horst block of Alboran Sea basement, the FT data suggest a similar thermal history for all the samples since early Miocene time, with rapid cooling at ~18–19 Ma succeeded by residence at <~60°C. The basement in Hole 976B is directly overlain by Serravallian (11–12 Ma) sediment. Preservation of the FT record indicates negligible (probably zero) track annealing in the basement subsequent to the early Miocene cooling. Such a restriction to a maximum temperature of ~60°C imposes limits on any additional sediment burial that might subsequently have been eroded.

TECTONIC IMPLICATIONS

The FT evidence for rapid cooling to 60°C at around 18–19 Ma is consistent with the Ar/Ar data reported by Kelley and Platt (Chap. 22, this volume) for cooling of the basement rocks through the 300°–450°C range at virtually the same time: the two sets of data suggest a very rapid exhumation and cooling event in the early Miocene. The dates are also very similar to those from similar high-grade metamorphic basement in the Betic Cordillera: Zeck et al. (1992), for example, report Rb/Sr, K/Ar, and Ar/Ar dates in the range 18–20 Ma; Monié et al. (1994) report Ar/Ar ages in the range 19–20 Ma; and Andriessen and Zeck (1996) report FT ages in the range 13–20 Ma. The metamorphic basement onshore is overlain in places by Aquitanian–Burdigalian sediment that is approximately coeval with these cooling ages (Bourgois et al., 1972, 1978; Aguador et al., 1990; Durand-Delga et al., 1993). The oldest sediment in adjacent parts of the West Alboran Basin may also be as old as late Aquitanian (Comas et al., 1992). It therefore appears very likely that the rapid exhumation of the basement coincided with the formation of the Alboran Sea basin, and that a primary mechanism of exhumation was tectonic extension and associated normal faulting.

Rapid exhumation results in significant advection of heat toward the earth's surface, steepening the geotherm, which complicates the

Table 1. Apatite fission-track data measured for Hole 976B Alboran Sea samples.

Sample	Depth (mbsf)	Rock type	No. of crystals	Dosimeter ρ_d	Dosimeter N_d	Spontaneous ρ_s	Spontaneous N_s	Induced ρ_i	Induced N_i	Age dispersion $P\chi^2$	Age dispersion RE%	Central age (Ma) ± 1σ	Mean track length (μm) ± 1 standard error	Mean track length standard deviation	No. of tracks
161-976B-															
77R-2 (Piece 3B)	685.83	Calc-silicate	(Inadequate apatite separated—no analysis possible.)												
83R-1 (Piece 11A)	727.66	Calc-silicate	(Apatites full of inclusions—no analysis possible.)												
92R-1 (Piece 10)	785.26	Calc-silicate	23	1.397	7745	0.203	149	2.335	1712	26	8.9	20.7 ± 1.8	14.25 ± 0.15	0.83	31
95R-2 (Piece 1D)	814.89	Gneiss	22	1.397	7745	0.139	104	1.540	1146	85	0.5	21.5 ± 2.2	14.23 ± 0.30	1.07	14
95R-2 (Piece 3)	815.3	Leucosome	20	1.397	7745	0.146	210	1.858	2670	97	0	18.6 ± 1.4	14.54 ± 0.13	1.26	96
96R-1 (Piece 4A)	823.05	Gneiss	20	1.397	7745	0.156	96	1.725	1064	61	4.8	21.4 ± 2.3	14.78 ± 0.21	1.01	24
97R-1 (Piece 7)	833.05	Gneiss	20	1.397	7745	0.144	81	1.723	972	87	0	19.7 ± 2.3	14.31 ± 0.23	1.11	24
97R-2 (Piece 1)	834.07	Schist/gneiss	20	1.397	7745	0.200	111	2.704	1499	27	16.5	17.8 ± 1.9	13.83 ± 0.24	1.29	29
97R-2 (Piece 22)	835.34	Granite	20	1.397	7745	0.200	170	2.445	2077	68	0.9	19.4 ± 1.6	14.30 ± 0.18	0.95	28
98R-1 (Piece 5)	842.36	Migmatite	20	1.397	7745	0.210	152	3.276	2370	95	0	15.2 ± 1.3	14.34 ± 0.20	1.11	33
98R-2 (Piece 2)	844.23	Neosome	20	1.397	7745	0.182	194	2.450	2611	91	0	17.8 ± 1.3	14.65 ± 0.14	1.15	71
102R-2 (Piece 10B)	882.76	Leucosome	20	1.397	7745	0.186	187	2.584	2593	69	0.2	17.1 ± 1.3	14.28 ± 0.11	0.91	65
104R-1 (Piece 10)	900.69	Calc-silicate	8	1.380	7252	0.168	36	1.936	416	96	0	19.2 ± 3.3	No lengths—many inclusions.		

Notes: Basement/sediment interface is 669.73 m below seafloor, $\rho_{d,s,i}$ = track densities ($\times 10^6$ tr cm^{-2}); $N_{d,s,i}$ = numbers of tracks counted. Spontaneous and induced: analyses by external detector method using 0.5 for the $4\pi/2\pi$ geometry correction factor. $P\chi^2$ is probability of obtaining χ^2 value for v degrees of freedom, where v = no. crystals – 1. Central age is a modal age, weighted for different precisions of individual crystals (see Galbraith and Laslett, 1993); ages calculated using dosimeter glass CN-5; analyst Carter ζ_{CN5} =339 calibrated by multiple analyses of IUGS-recommended apatite and zircon age standards (see Hurford, 1990).

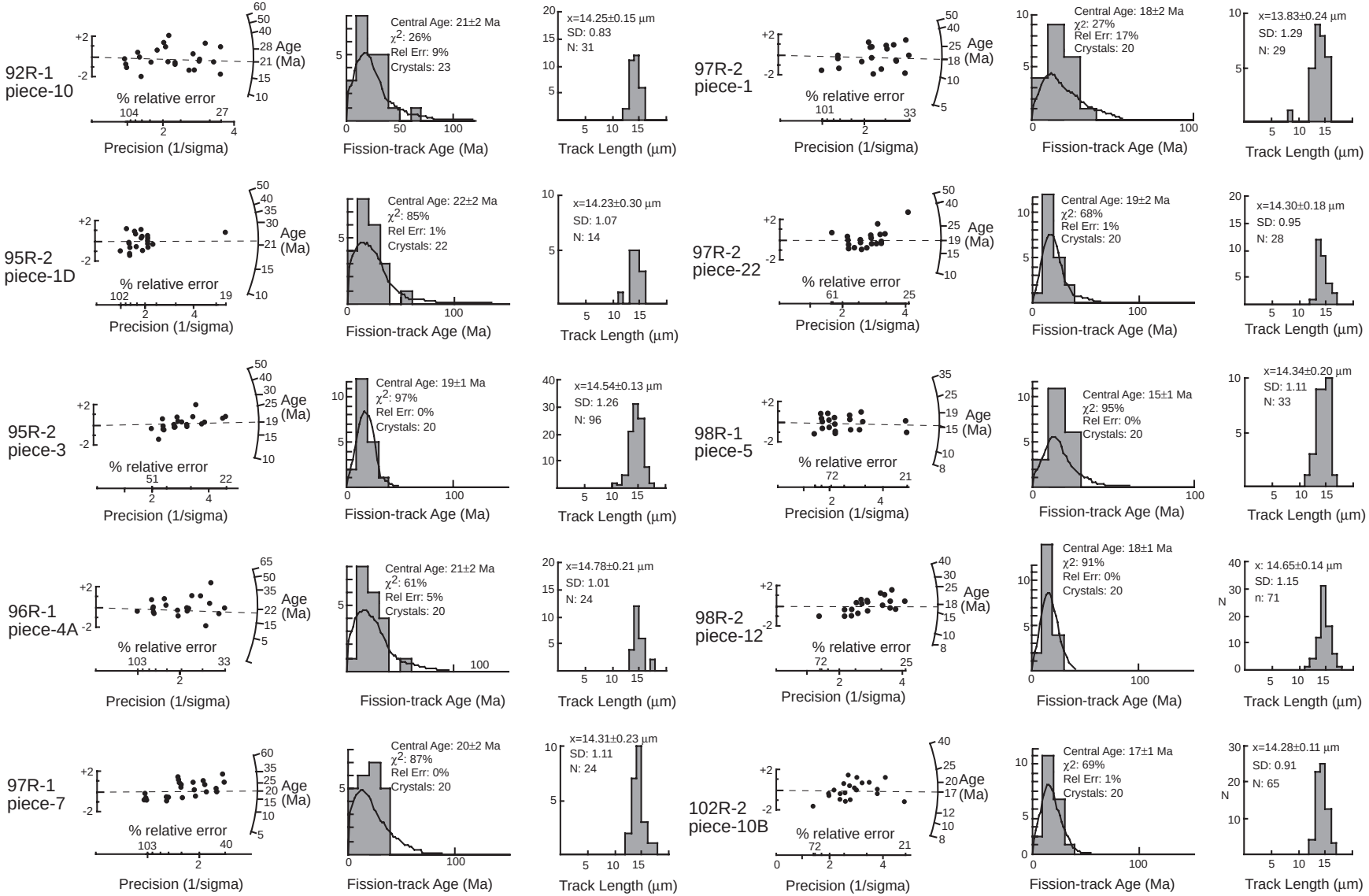

Figure 1. Fission-track ages and track-length distributions measured for Alboran Sea samples from Hole 976B. Intercepts on the circular age scale of the radial plots (left) yield individual crystal ages and result from linear extrapolation from the left-hand origin through each crystal age. The position on the x-scale is determined by the precision of each individual crystal age (Galbraith, 1990). Dashed lines show sample stratigraphic ages.

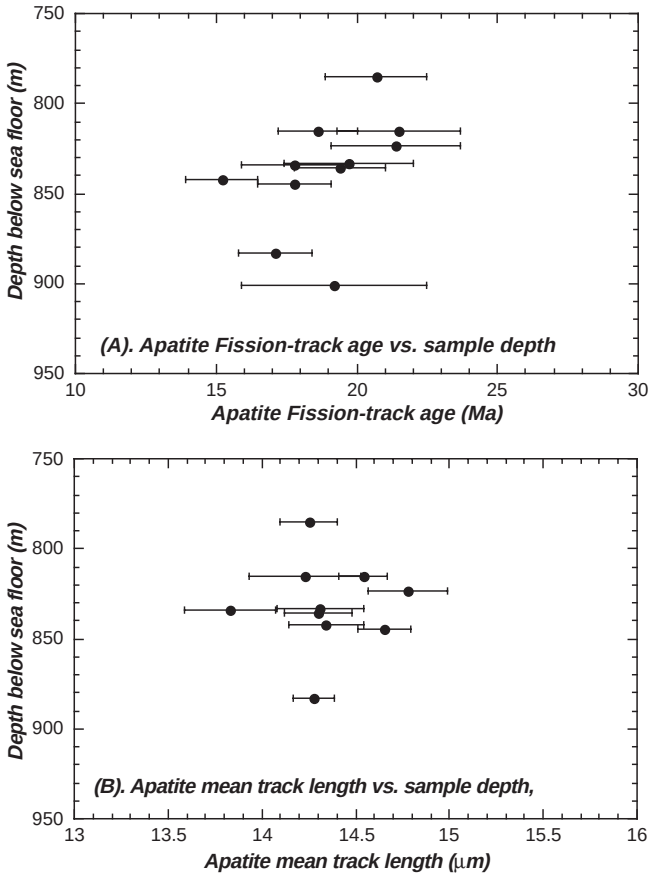

Figure 2. Measured apatite fission-track ages **(A)** and mean track lengths **(B)** plotted vs. depth of sample from Hole 976B in the Alboran Sea basement. Error bars represent experimental uncertainties and are 1σ.

calculation of exhumation rates from cooling rates. Bearing this in mind, cooling of Site 976 basement through the PAZ probably occurred within the top 1–2 km of the crust, and represents perhaps 1 km of exhumation. The site is located on a horst block with a vertical relief >2000 m (see Watts et al., 1993, for a seismic profile across the block), thus it is likely that this phase of exhumation was directly related to the creation of the present basement morphology in the area. It also means that calculation of a precise exhumation rate from the FT data would be further complicated by lateral heat flow in both horizontal dimensions, and for this reason we have not attempted it.

The absence of sediment older than Serravallian at Site 976 suggests that the horst block may have been emergent until that time, which leaves open the possibility that at least part of the final exhumation of the basement to the pre-Serravallian surface was accomplished by erosion.

ACKNOWLEDGMENTS

This study was funded by grant number GR3/10828 from the Natural Environmental Research Council of Great Britain. We thank J. Bourgois, M. Comas, and G. Omar for helpful reviews.

REFERENCES

Aguador, R., Feinberg, H., Durand-Delga, M., Martín-Algarra, A., Esteras, M., and Didon, J., 1990. Nuevas datos sobre la edad de las formaciones miocenas trasgresivas sobre las Zonas Internas béticas: la formación de San Pedro de Alcántara (Provincia de Málaga). *Rev. Soc. Geol. Esp.*, 3:79–86.

Andriessen, P.A.M., and Zeck, H.P., 1996. Fission-track constraints on timing of Alpine nappe emplacement and rates of cooling and exhumation, Torrox area, Betic Cordilleras, S. Spain. *Chem. Geol.*, 131:199–206.

Bourgois, J., 1978. La transversale de Ronda, Cordillères bétiques, Espagne: donnés géologiques sur une modèle d'évolution de l'arc de Gibraltar. *Ann. Sci.Univ. Besançon, Geol. Fasc.*, 30.

Bourgois, J., Chauve, P., Magne, J., Monnot, J., Peyre, Y., Rigo, E., and Rivière, M., 1972. La formation de las Millanas: série Burdigalienne trangressive, sur les zones internes des Cordillères bétiques occidentales (region d'Alozaina-Tolox, province de Malaga, Espagne). *C. R. Acad.Sci. Ser. 2*, 275:169–172.

Comas, M.C., García-Dueñas, V., and Jurado, M.J., 1992. Neogene tectonic evolution of the Alboran Basin from MCS data. *Geo-Mar. Lett.*, 12:157–164.

Durand-Delga, M., Feinberg, H., Magné, J., Olivier, P., and Anglada, R., 1993. Les formations oligo-miocène discordantes sur les Malaguides et les Alpujarrides et leurs implications dans l'évolution géodynamiques des Cordillères bétiques (Espagne) et de la Méditerranée d'Alboran. *C. R. Acad. Sci. Ser. 2*, 317:679–688.

Galbraith, R.F., 1981. On statistical models for fission track counts. *Math. Geol.*, 13:471–478.

————, 1990. The radial plot: graphical assessment of spread in ages. *Nucl. Tracks*, 17:207–214.

Galbraith, R.F., and Laslett, G.M., 1993. Statistical models for mixed fission-track ages. *Nucl. Tracks Radiation Measure.*, 21:459–470.

Gallagher, K., 1995. Evolving temperatures histories from apatite fission-track data. *Earth Planet. Sci. Lett.*, 136:421–435.

Gleadow, A.J.W., 1981. Fission track dating methods: what are the real alternatives? *Nucl. Tracks*, 5:3–14.

Gleadow, A.J.W., Duddy, I.R., Green, P.F., and Lovering, J.F., 1986. Confined track lengths in apatite—a diagnostic tool for thermal history analysis. *Contrib. Mineral. Petrol.*, 94:405–415.

Green, P.F., and Hurford, A.J., 1984. Thermal neutron dosimetry for fission track dating. *Nucl. Tracks*, 9:231–241.

Hurford, A.J, 1990. Standardization of fission track dating calibration: recommendation by the Fission Track Working Group of the I.U.G.S. Subcommission on Geochronology. *Chem. Geol.*, 80:171–178.

Hurford, A.J., and Green, P.F., 1982. A user's guide to fission-track dating calibration. *Earth Planet. Sci. Lett.*, 59:343–354.

————, 1983. The zeta age calibration of fission-track dating. *Chem. Geol.*, 41:285–317.

Laslett, G.M., Green, P.F., Duddy, I.R., and Gleadow, A.J.W., 1987. Thermal annealing of fission tracks in apatite—a quantitative analysis. *Chem. Geol.*, 65:1–15.

Lewis, C.L.E., Green, P.F., Carter, A., and Hurford, A.J., 1992. Elevated K/T palaeotemperatures throughout Northwest England: three kilometres of Tertiary erosion? *Earth Planet. Sci. Lett.*, 112:131–145.

Monié, P., Torres-Roldán, R.L., and García-Casco, A., 1994. Cooling and exhumation of the western Betic Cordilleras, $^{40}Ar/^{39}Ar$ thermochronological constraints on a collapsed terrane. *Tectonophysics*, 238:353–379.

Platt, J.P., Soto, J.I., Comas, M.C., and Leg 161 Shipboard Scientists, 1996. Decompression and high-temperature–low-pressure metamorphism in the exhumed floor of an extensional basin, Alboran Sea, Western Mediterranean. *Geology*, 24:447–450.

Platt, J.P., and Vissers, R.L.M., 1989. Extensional collapse of thickened continental lithosphere: a working hypothesis for the Alboran Sea and Gibraltar Arc. *Geology*, 17:540–543.

Shipboard Scientific Party, 1996. Site 976. *In* Comas, M.C., Zahn, R., Klaus, A., et al., *Proc. ODP, Init. Repts.*, 161: College Station, TX (Ocean Drilling Program), 179–297.

Watts, A.B., Platt, J.P., and Buhl, P., 1993. Tectonic evolution of the Alboran Sea Basin. *Basin Res.*, 5:153–177.

Working Group for Deep Seismic Sounding in the Alboran Sea 1974, 1978. Crustal seismic profiles in the Alboran Sea: preliminary results. *Pageophysics*, 116:167–180.

Zeck, H.P., Monié, P., Villa, I.M., and Hansen, B.T., 1992. Very high rates of cooling and uplift in the Alpine belt of the Betic Cordilleras, southern Spain. *Geology*, 20:79–82.

Date of initial receipt: 23 April 1997
Date of acceptance: 1 October 1997
Ms 161SR-213

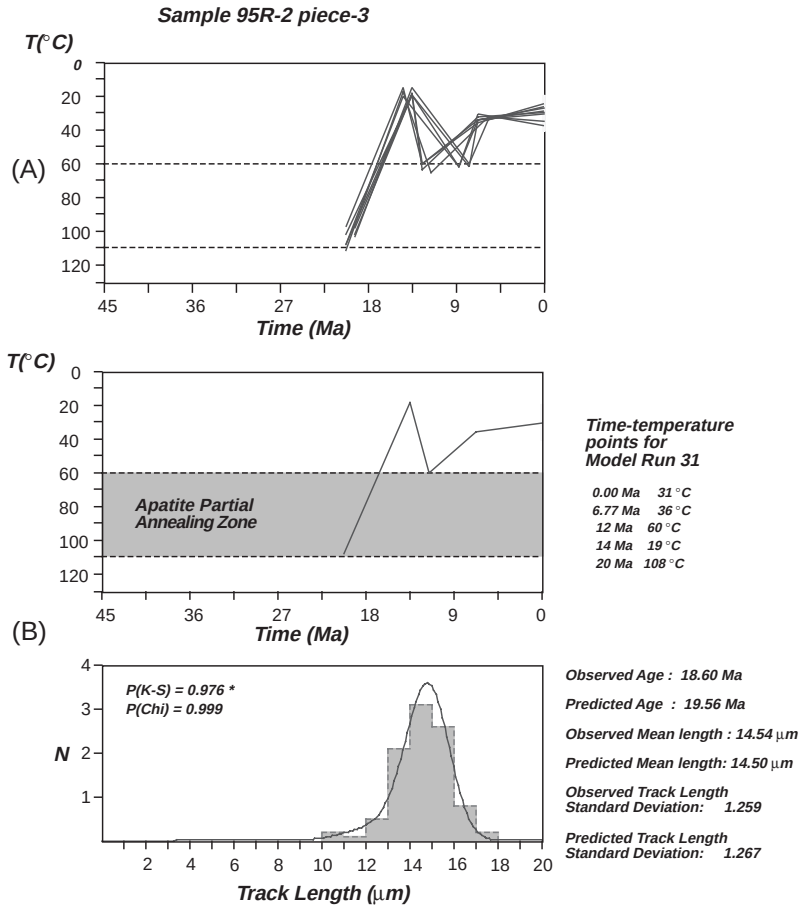

Figure 3. Time-temperature histories that yield best-fit of predicted results to measured fission-track lengths and ages for Sample 161-95R-2 (Piece 3). **A.** Ten better fitting results. **B.** The best-fit run #31, one of 5000 runs modeled using a Monte Carlo genetic algorithm approach (Gallagher, 1995) and the Laslett et al. (1987) apatite track-annealing description. Note that detail in the tT pattern at <60°C is unconstrained because no significant track annealing occurs at these temperatures.

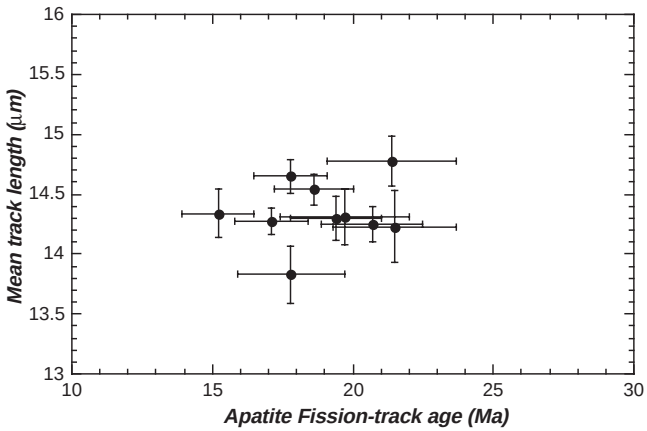

Figure 4. Measured apatite fission-track age plotted vs. measured mean track length for Alboran Sea basement samples. Error bars are analytical uncertainties and are 1σ.